

# Changing monsoon and midlatitude circulation interactions over the Western Himalayas and possible links to occurrences of extreme precipitation

P. Priya<sup>1,2</sup> · R. Krishnan<sup>1</sup> · Milind Mujumdar<sup>1</sup> · Robert A. Houze Jr.<sup>3,4</sup>

Received: 27 August 2016 / Accepted: 14 November 2016  
© Springer-Verlag Berlin Heidelberg 2016

**Abstract** Historical rainfall records reveal that the frequency and intensity of extreme precipitation events, during the summer monsoon (June–September) season, have significantly risen over the Western Himalayas (WH) and adjoining upper Indus basin since 1950s. Using multiple datasets, the present study investigates the possible coincidences between an increasing trend of precipitation extremes over WH and changes in background flow climatology. The present findings suggest that the combined effects of a weakened southwest monsoon circulation, increased activity of transient upper-air westerly troughs over the WH region, enhanced moisture supply by southerly winds from the Arabian Sea into the Indus basin have likely provided favorable conditions for an increased frequency of certain types of extreme precipitation events over the WH region in recent decades.

**Keywords** Extreme precipitation events · Western Himalayas · Indus basin · Changes in background climatology

**Electronic supplementary material** The online version of this article (doi:[10.1007/s00382-016-3458-z](https://doi.org/10.1007/s00382-016-3458-z)) contains supplementary material, which is available to authorized users.

✉ R. Krishnan  
krish@tropmet.res.in

<sup>1</sup> Centre for Climate Change Research, Indian Institute of Tropical Meteorology, Pune 411 008, India

<sup>2</sup> Department of Atmospheric and Space Science, Savitribai Phule Pune University, Pune, India

<sup>3</sup> University of Washington, Seattle, WA, USA

<sup>4</sup> Pacific Northwest National Laboratory, Richland, WA, USA

## 1 Introduction

Rainfall observations from stations in Pakistan indicate increasing trends in extreme daily precipitation occurrences over northeastern areas of Pakistan during the 1950–2010 and the pattern of increasing trends appears to be more prominent during the spring and summer seasons, as compared to the winter months (Hussain and Lee 2013). Gridded rainfall datasets also reveal the overall increasing trends in daily precipitation extremes in this region of the Western Himalayas (WH) (see Wang et al. 2011; Malik et al. 2016). Although the mean summer monsoon precipitation tends to be relatively low over northern Pakistan and Indus basin, in comparison with the abundant rains that occur over the plains of Central and North India and the Central-Eastern Himalayan (CEH) region, the rainfall variability is rather high over the WH region. Moreover, the climate of WH is somewhat typical of mountainous semiarid to arid environment and the region is highly vulnerable to extreme rainfall events (e.g., Saeed et al. 2011; Salma et al. 2012; Rasmussen et al. 2015). The WH region is also influenced by winter precipitation in the form of both snow and rain, so that snow/glacier melt and river runoff are important sources of freshwater for the region (e.g. Immerzeel et al. 2010). While some Himalayan glaciers are reported to be losing mass in recent decades, the Karakoram glaciers show anomalous behavior in terms of snow cover and ice budgets (Gardelle et al. 2012; Bolch et al. 2012; Kapnick et al. 2014; Hasson et al. 2014). Any change in the mass balance of the Himalayan glaciers has serious implications on the river runoff in one of the most densely populated and socio-economically complex regions of the world (Bolch et al. 2012; Hasson et al. 2014). In addition, river flows in this region are highly susceptible to rainfall variations, so that

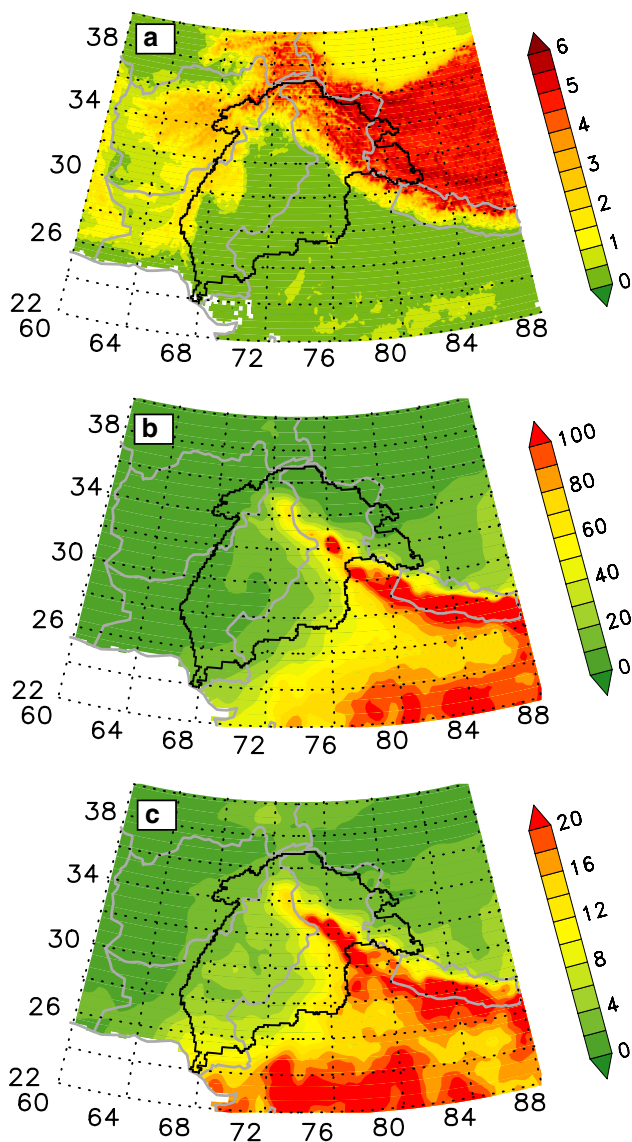


**Fig. 1** **a** Elevation map (unit: km) of the western Himalayan region. **b** Mean total seasonal June–September (JJAS) rainfall (cm) from APHRODITE. **c** SD (cm) of total seasonal rainfall. Elevation data is taken from global multi-resolution Terrain elevation data 2010 (GMTED2010). Indus basin is shown by the thick black contour

any change in precipitation pattern over the mountainous areas can create far-reaching impacts on fresh water availability in downstream areas (Nijssen et al. 1997; Arnell 2003; Messerli et al. 2004). In addition, the steep topography over this region can exacerbate surface runoff during heavy rain events, in turn leading to landslide and flooding (Bookhagen and Burbank 2010).

Being located over the western flank of the South Asian Monsoon system, the summer monsoon rains over the WH account for nearly 50–60% of the annual rainfall. Figure 1 shows maps of topographic elevation, the mean and standard deviation (SD) of JJAS rainfall over the

WH region and adjoining areas near the western flank of the Asian monsoon system. The Indus river basin spans a large area of about  $1.01 \times 10^6 \text{ km}^2$  that covers India, Pakistan, Afghanistan and China (thick black border). The accumulated seasonal summer monsoon rainfall amounts across the WH range from low values ( $<10 \text{ cm}$ ) to high precipitation amounts  $>100 \text{ cm}$  over central-eastern Indus basin. Although the mean rainfall averaged over the WH region is rather low ( $\sim 12 \text{ cm}$ ), the variability of accumulated precipitation is high especially in the central Indus basin ( $>6 \text{ cm}$ ). Changes in large-scale circulation pattern and moisture transport can significantly influence convection over this area and trigger extreme rainfall events (see Houze et al. 2007; Wang et al. 2011; Mujumdar et al. 2012; Priya et al. 2015). Moreover the summer rainfall variability in this region is closely linked to circumglobal teleconnection patterns, which are known to influence the South Asian monsoon variability through modulation of the upper tropospheric anticyclone (Ding and Wang 2005, 2007; Saeed et al. 2011). While precipitation extremes are generally expected to increase in a warming environment, increases in atmospheric water vapor content alone cannot explain changes in intense rain events due to their strong dependence on vertical motions (Sugiyama et al. 2010) and precipitation efficiency of different storm types. Inadequate representations of precipitation processes over the Indus basin often pose great challenges in hydrologic modeling (Hasson et al. 2013). Complex network analysis of precipitation data reveals that extreme rainfall occurrence over Northwest Pakistan and adjoining India have strong connectivity with other regions in the Asian monsoon domain (Malik et al. 2012).

Areas in the northern Pakistan and Indus basin witnessed a series of major cataclysmic flood events in the recent past. These floods have arisen from heavy precipitation in the summer monsoon seasons since 2010, including the Leh flash flood of 2010, the cataclysmic Pakistan floods of 2010, 2011 and 2012, the Uttarakhand floods in northern India during 2013 and the Jammu–Kashmir floods in 2014. Literature on heavy rain events in the Himalayan and nearby regions include Houze et al. (2007, 2011), Medina et al. (2010), Hong et al. (2011), Webster et al. (2011), Lau and Kim (2012), Rasmussen and Houze (2012), Martius et al. (2013), Mujumdar et al. (2012), Dobhal et al. (2013), Kumar et al. (2014), Vellore et al. (2015), Priya et al. (2015), Rasmussen et al. (2015), and Lotus (2015). Some of these studies (e.g. Rasmussen et al. 2015) point to a characteristic synoptic-scale pattern characterized by strong ridge conditions over the Tibetan plateau, which together with a monsoonal low over northern India produce strong moist flow from the Bay of Bengal and/or Arabian Sea. Other studies point out the linkage of the WH heavy precipitation episodes to upper-level midlatitude baroclinic

troughs extending southward to the Himalayas and interacting with the monsoon low-pressure system over northern India so as to produce an anomalous moisture flux large enough to support storms capable of producing floods (e.g., Vellore et al. 2015; Houze et al. 2016). Krishnamurti et al. (2016) highlighted the role of moisture transport from the Bay of Bengal and Arabian Sea into the heavily raining clouds over the Uttarakhand region resulting in large build up of buoyancy and strong vertical accelerations during the 2013 extreme rain event. In some storms that produce floods in the Himalayan region, the clouds take the form of deep mesoscale convective systems (Houze et al. 2011; Rasmussen and Houze 2012; Kumar et al. 2014; Rasmussen et al. 2015). In other cases (Houze et al. 2016), the storms have only moderate convective elements embedded in widespread persistent largely non-convective precipitating clouds. The different nature of storms indicates that the primary factor determining whether storms can produce extreme precipitation and flooding in this region is the formation of strong anomalous moisture supply. Climate models have major challenges in simulating the mean summer monsoon precipitation around the Indus basin and adjoining areas (Hasson et al. 2016). Therefore, it is worth exploring possible connections between large-scale circulation variability in relation to moisture supply and the observed increasing trend of extreme daily rain intensity over parts of Pakistan and Northwest Himalaya (Hussain and Lee 2013; Malik et al. 2016).

The present study focuses on the type of storm that is characterized by a baroclinic trough in the westerlies extending southward to the Himalayas. The objective of this study is to determine whether the observed increasing trend of extreme daily rain occurrences over the WH coincides with changing background circulation over the South Asian monsoon region and adjoining areas; i.e., whether large-scale circulation changes have increased the likelihood of this type of extreme rain event over the western Himalayan watersheds. We do not attempt to distinguish whether individual events are intensely convective or have the character of stable-to-neutral streams of moisture lifted over the mountains. Rather, we pay attention to the possible correspondence of statistics of heavy rainfall over the WH region and those of the large-scale background circulation. More specifically, we aim to identify the trend in occurrence of troughs extending southward over the Himalayan region and determine if such behavior of the large-scale circulation corresponds to major rain events in the region.

Various studies have documented significant decreasing trends in the seasonal monsoon rainfall over India and associated changes in the background monsoon circulation (e.g., Guhathakurta and Rajeevan 2008; Krishnan et al. 2013, 2015; Joseph and Simon 2005; Sathiyamoorthy 2005; Abish et al. 2013; Singh et al. 2014 and others). Weakening

of the South Asian monsoon (SAM) meridional overturning circulation can facilitate generation of quasi-stationary anomaly patterns over the subtropics and mid-latitudes (Krishnan et al. 2009, 2015; Krishnan and Sugi 2001). Srivastava et al. (2014) noted that the summer time energetics of extra-tropical circulation significantly changed during post 1980s as compared to earlier decades. Latif et al. (2016) examined trends in the June–September seasonal rainfall over South Asia for the period (1951–2012) and reported a dipole pattern of positive trend over the Indo-Pak region and negative trend over the core monsoon region of north-central India. They suggested that extra-tropical circulation patterns like the circumglobal teleconnection (CGT) can influence mean monsoon rainfall trends over Pakistan under the influence of moisture transport over the Arabian Sea. The Latif et al. (2016) study focused on monthly and seasonal rainfall, but not on daily precipitation extremes. Moreover, as discussed above, moisture flux associated with heavy rain episodes over the WH can arise from more than one type of midlatitude synoptic-scale flow pattern (notably, a ridge over Tibet or a trough in the westerlies extending southward to the WH). The question arises as to whether the increasing occurrence of extreme precipitation events over the WH region has any connection with changes in the SAM circulation, in particular the activity of upper-level westerly troughs over the region. To explore the possible link of WH heavy rain events to changes in the general circulation, we have stratified the occurrence of events in terms of the so-called Webster–Yang index (WYI) which provides a dynamical measure of the intensity of the large-scale monsoon circulation (Webster and Yang 1992). The details are given in Sect. 3.

## 1.1 Data

We utilize the Asian Precipitation Highly Resolved Observational Data Integration Towards Evaluation (APHRODITE) daily precipitation datasets (Yatagai et al. 2012) at fine resolution ( $0.25^\circ \times 0.25^\circ$ ) for the time period 1951–2007. We have also examined global rainfall over the tropics derived from the TRMM (Tropical Rainfall Measuring Mission) satellite and other rainfall estimates (3B42) precipitation data for the period 1998–2007 (Huffman et al. 2007). For meteorological variables, we used the European Centre for Medium Range Weather Forecasts (ECMWF) ERA40 (1958–2001) reanalysis (Uppala et al. 2005) and ERA Interim reanalysis (1979–2013) (Uppala et al. 2008). We have also examined daily winds for the period (1951–2007) using the National Center for Environmental Prediction (NCEP) reanalysis data (Kistler et al. 2001). In addition, sea surface temperature (SST) and mean sea level pressure (SLP) data for the period 1958–2001 are analyzed based on the HadISST (Rayner et al. 2003) and HadSLP2 (Allan and



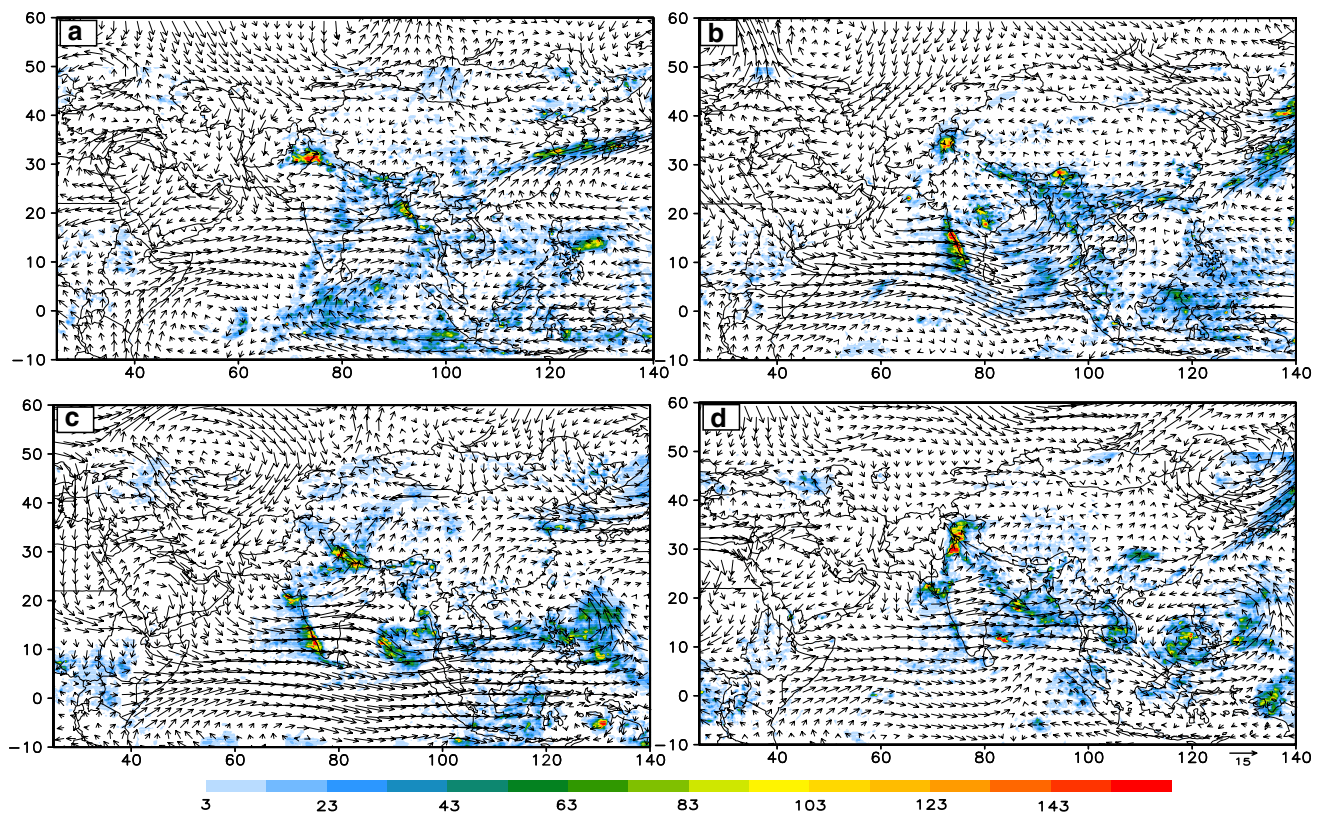


**Fig. 2** Precipitation ( $\text{mm day}^{-1}$ ) and 700 hPa winds ( $\text{ms}^{-1}$ ) for the heavy rainfall events of **a** 12 July 2010, **b** 29 July 2010, **c** 17 June 2013 and **d** 04 September 2014. References for these four events

are from Hong et al. (2011), Rasmussen et al. (2015), Vellore et al. (2015) and Lotus (2015) respectively. Precipitation and wind data are from TRMM3B42 estimates and ERA Interim reanalysis

Ansell 2006) datasets respectively. Global multi-resolution terrain elevation data 2010 (Danielson and Gesch 2011) is used to show the topographic features of WH region.

## 2 Understanding heavy precipitation over the WH region

The present diagnostic analysis is focused on the boreal summer monsoon season (June–September, JJAS). Episodes of strong convective motions and heavy rainfall in the WH during the monsoon involve moisture transport from the Arabian Sea and/or Bay of Bengal (Hong et al. 2011; Houze et al. 2007; Medina et al. 2010; Rasmussen et al. 2015; Priya et al. 2015). Figure 2 shows examples of circulation patterns at 700 hPa over the tropics and extra-tropics that were prevailing when heavy rainfall (intensity  $> 200 \text{ mm day}^{-1}$ ) occurred over the WH. These examples include the case with westerly trough around the vicinity of Pakistan (e.g., 12 July 2010), a continental-scale cyclonic circulation over India and easterly flow from the Bay of Bengal area (e.g., 29 July 2010), prominent trough in the subtropical westerlies extending from

the mid-latitudes almost over the WH region (e.g., 17 June 2013, 05 September 2014). The westerly trough on 17 June 2013 connected with the monsoon low over north India to produce the strong moist flow in that case (Houze et al. 2016). The Uttarakhand case was a well-defined example of the type of event analyzed by Vellore et al. (2015). They found that a common pattern associated with heavy rainfall over the WH is of a southward extending trough interacting with a west-northwest propagating monsoon low. The cases illustrated in Fig. 2 all exhibit a trough-like feature in the westerlies at 700 hPa extending from the mid-latitudes into the WH region. This trough-like feature in the upper-level extra-tropical westerlies is also discernible at the 850 hPa level (Auxiliary Fig. A1). However, several notorious floods were not associated with any southward intrusion of a trough in the midlatitude westerlies (Rasmussen et al. 2015); indeed, ridge conditions dominated north of the Himalayas. In these cases, southerly winds from the Arabian Sea and/or Bay of Bengal can trigger deep convection and supply mesoscale convective systems over the hot arid regions of northwest India and Indus basin by accumulating instability via surface heating which is eventually released by orographically induced lifting over the

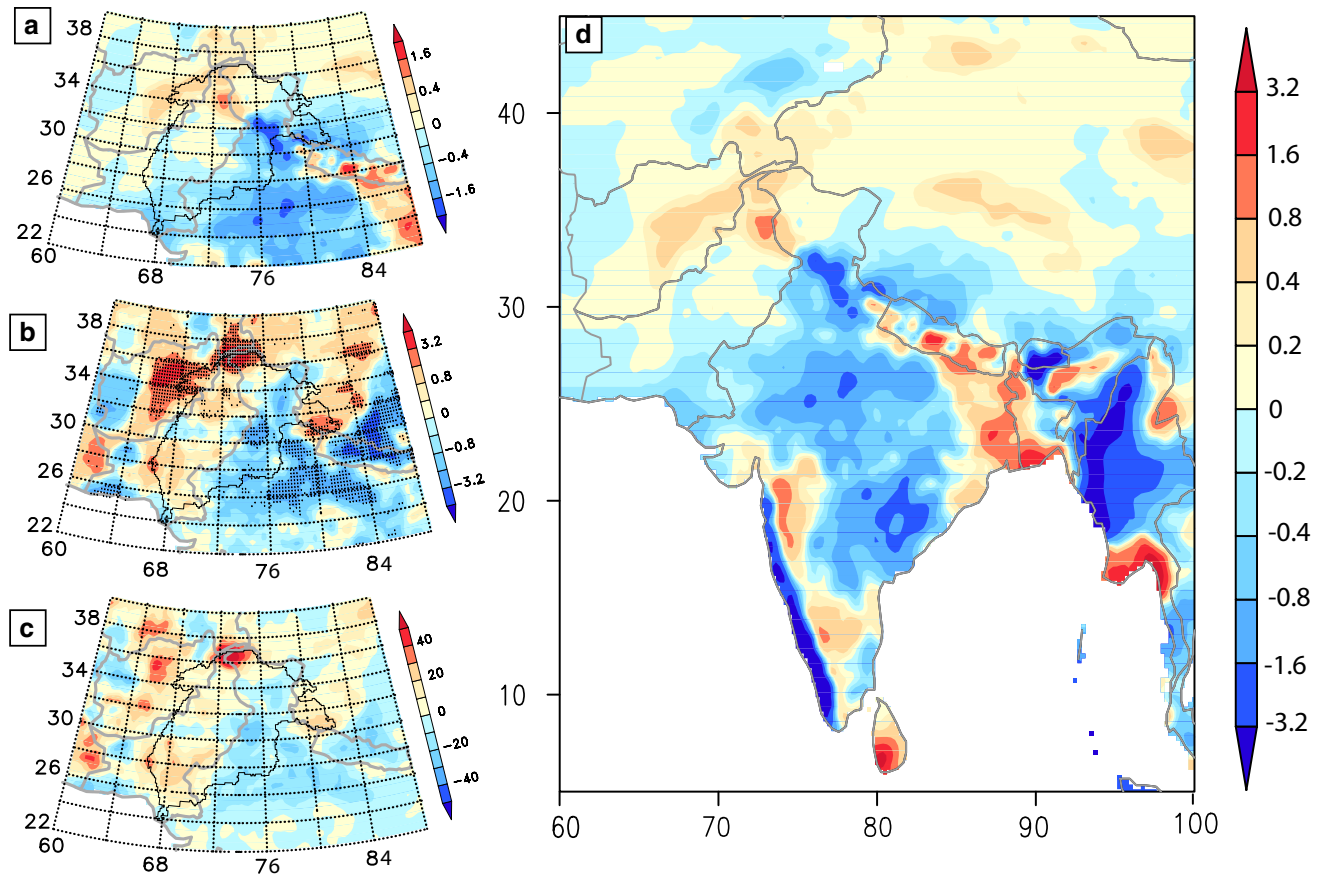


**Fig. 3** Spatial map showing linear trend of **a** JJAS rainfall rate for the period 1951–2007 [units: mm day<sup>-1</sup> (57 year)<sup>-1</sup>] over Western Himalayas and adjoining areas, **b** Count of extreme rainfall events [rainfall > 99th percentile; unit: count (57 year)<sup>-1</sup>]. Trend values exceeding the 95% confidence level based on a student's *t* test (Santer et al. 2000) are marked with *dots*, **c** Percentage contribution of daily precipitation extremes to total seasonal rainfall [unit: percentage (57 year)<sup>-1</sup>], **d** Same as (a) but for the Indian region. The analysis is

based on the APHRODITE daily gridded rainfall data sets at  $0.25^\circ \times 0.25^\circ$  resolution for the period 1951–2007. The opposite behavior of trends over western and eastern portions of northern near-Himalayan region in (d) suggests a shift in the nature of the precipitation. Houze et al. (2007, 2016) find that the precipitation in the western portion tends to be more intensely convective without stratiform components, while that in the eastern zone is often less intense with large stratiform regions

Himalayan foothills (e.g., Sawyer 1947; Houze et al. 2007; Medina et al. 2010). The purpose of this study is not to provide a common explanation for the individual cases of heavy rainfall events over the WH region. Rather, we aim to gain statistical insight how one category of storm contributes to an apparently increasing trend of heavy rainfall over the WH during the last few decades.

## 2.1 Long-term trends in monsoon rainfall and extreme precipitation over WH

Spatial heterogeneity in long-term trends of the monsoon rainfall over the Indian region has been documented by earlier studies (Tank et al. 2006; Krishnamurthy et al. 2009; Ghosh et al. 2011). The spatial map of linear trend of JJAS seasonal rainfall for the period 1951–2007 shows a significant positive trend over the mountainous regions of

northern Indo-Pakistan and Afghanistan (Fig. 3a). It must be mentioned that changes in summer-time precipitation can also have implications for glacier mass balance, particularly in the upper Indus basin (Hasson et al. 2014). It is further interesting to note a decreasing trend in the JJAS rainfall over the lower Indus basin and adjacent regions of north and Central India (Fig. 3a). Further discussion related to spatially non-homogeneous rainfall trends will be conferred in subsequent sections.

We have further examined changes in the frequency of daily precipitation extremes over the WH region using the APHRODITE daily gridded precipitation dataset. For this purpose, year-by-year counts of the number of precipitation events exceeding the 99th percentile were first determined at each grid-point for every JJAS monsoon season during 1951–2007. From the time-series of frequency counts of extreme precipitation occurrences, we then calculated the

linear trend for the period 1951–2007 at each grid-point (see Fig. 3b). It is apparent that more than 65% of the area of the Indus basin exhibits a positive trend in the frequency of occurrence of daily precipitation extremes. The positive trend over the upper Indus basin in Fig. 3b is nearly co-located with the positive trend in JJAS rainfall (Fig. 3a), suggesting a significant role of daily precipitation extremes on the trend in seasonal rainfall over this region. Using data from TRMM, Houze et al. (2007, 2016) have identified this region as one where deep intense convective elements are most likely to form. These deep convective elements are triggered by passage over the lower foothills after low-level moist air has traversed the hot land surface of the Thar Desert and increased its CAPE while being capped by dry subsiding flow off the Afghan Plateau (Medina et al. 2010). The data presented here suggests that the occurrence of such convection has increased over time. The increase in contribution of daily precipitation extremes to the JJAS seasonal total precipitation during 1951–2007 is more than 20% covering an area of about 35% of the whole Indus basin (Fig. 3c). We further note that the negative trend over the lower Indus basin and northwest India (Fig. 3b) is rather similar to that of the JJAS seasonal precipitation counterpart in Fig. 3a. Another important aspect is that the region of greatest significant increasing trend of daily precipitation extremes (Fig. 3b) coincides with highly elevated regions of the WH, which is noteworthy from the climate change perspective because of the elevation dependency of the climate warming signal (Giorgi et al. 1997; Rangwala and Miller 2012; Rangwala et al. 2013).

It must be recognized that interpretation of long-term changes in extreme events can be affected by changes in methods or reporting of observations. While this is a challenging issue, evidences based on long-term rainfall records from stations in Pakistan lend support to the increasing trend of precipitation extremes in the region (Hussain and Lee 2013). Furthermore, to ensure reliability of our analysis we have compared daily precipitation extremes over the WH region using the APHRODITE and TRMM-3B42 datasets for the common period (1998–2007) (Auxiliary Fig. A2). We find that the time-series of the total count of precipitation extremes over WH region for the common period (1998–2007) from the two datasets are strongly correlated ( $r = 0.95$ ). Section 3.1 presents further discussion of the analysis of daily precipitation extremes.

To better understand the non-homogeneous pattern of trends, we performed an empirical orthogonal function (EOF) analysis on the year-wise frequency counts of extreme precipitation events. EOF analysis has been extensively used by various investigators to extract the dominant modes of spatio-temporal variability (Hsiung and Newell 1983; Barbosa and Andersen 2009; Compo and Sardeshmukh 2010; Mishra et al. 2012). Spatial patterns of the three dominant EOFs of the frequency counts of daily precipitation extremes are shown in

Fig. 4a–c. The time-series of the corresponding three principal components (PC) and the year-by-year count of daily precipitation extremes over the WH region (64°E–76°E, 32°N–38°N) are shown in Fig. 4d. The time-series of the number of daily precipitation extremes shows a clear upward trend. It is also seen that the second mode (EOF2) has positive loading over the Upper Indus basin and the corresponding time-series (PC2) exhibits a prominent upward trend at the 0.001 significance level. On the other hand, the 1st and 3rd modes (EOF1/PC1 and EOF3/PC3) do not exhibit positive trend over the upper Indus basin (Fig. 4). It is also important that the EOF2 pattern shows remarkable similarity with the spatial pattern of trend in frequency of daily precipitation extremes depicted in Fig. 3b and the two have a spatial correlation of 0.94. Furthermore, the PC2 time-series (red line) and the time-series of frequency of daily precipitation extremes (blue line) over the WH region are strongly correlated ( $r = 0.79$ ). Because of these correlations, we take the PC2 time-series, which captures the evolution of the spatially heterogeneous trend pattern, as the index for extreme precipitation events over the Indus basin for further analysis. It is interesting to note that the EOF2 pattern shows negative loadings over northern India, which suggest that the trends in the frequency of precipitation extremes are opposite between the northwest Indus basin and northern India. The negative loadings of EOF2 over northern India, moreover, are consistent with the results of Krishnamurthy et al. (2009) who noted a decreasing trend in the frequency and intensity of daily precipitation extremes over north India during the period 1951–2003. A likely physical interpretation of EOF2/PC2 is discussed later in Sect. 4. Corroborative support for the increasing trend of daily precipitation extremes during the post-1950s over the WH is also evident in the frequency of daily synoptic-scale 500 hPa vertical velocities in the ERA-Interim and ERA-40 reanalyses that exceed the 95th and 99th percentile (Fig. 5). The statistical coincidence of increasing trends of daily precipitation extremes and strong upward velocities, as seen in reanalysis fields, indicate that support from large-scale lifting is beneficial to the release of precipitation. However, the fact remains that the precipitation may come in different ways—deep intense convection, synoptically forced circulation patterns, orographic lifting of stable or moist neutral airflows, or the stratiform regions of mesoscale convective systems.

### 3 Link between changes in precipitation extremes and large-scale circulation

#### 3.1 Association with anomalies of wind, pressure, and SST

Here we examine the connection between the large-scale circulation and extreme rainfall activity over the WH.



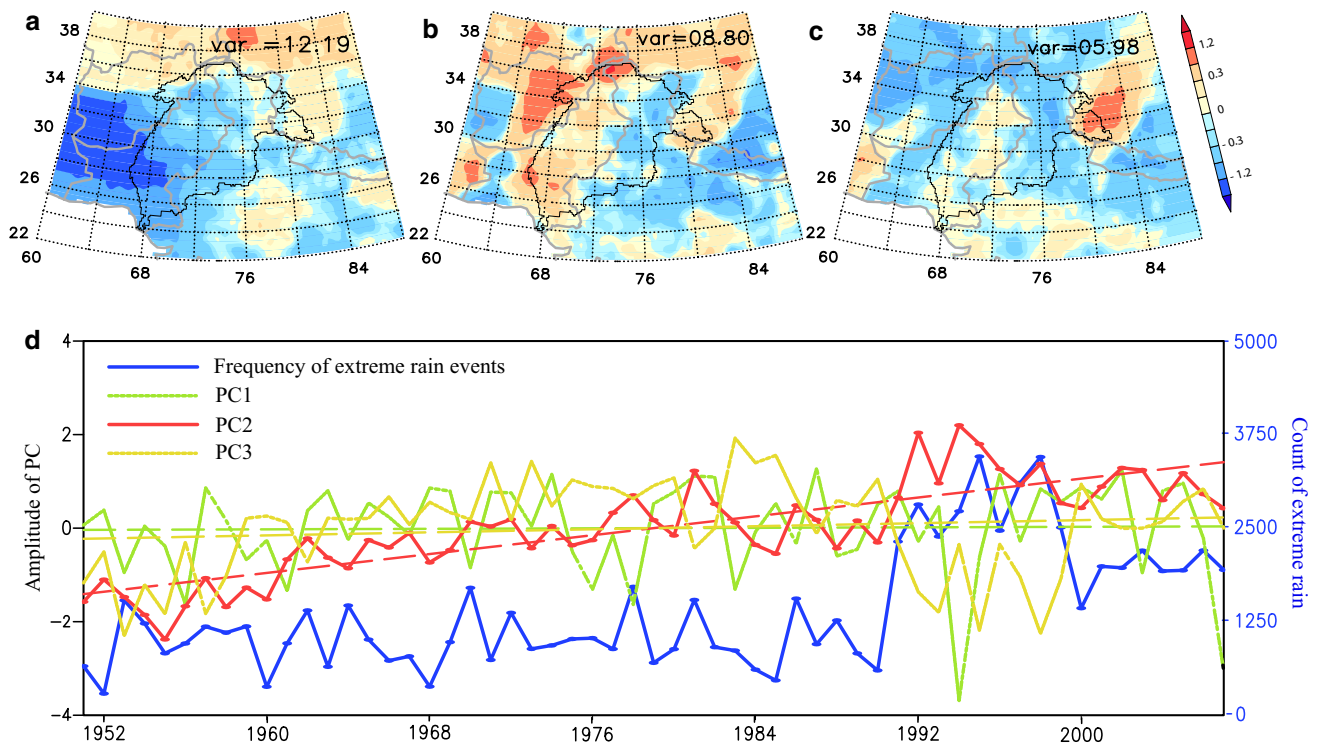


**Fig. 4** Spatial maps of the **a** first, **b** second, **c** third EOF pattern of frequency of extreme rain events for the period 1951–2007 based on APHRODITE rainfall dataset. The variance explained by the three EOF modes is shown in the figures. **d** Time series of inter-annual variations

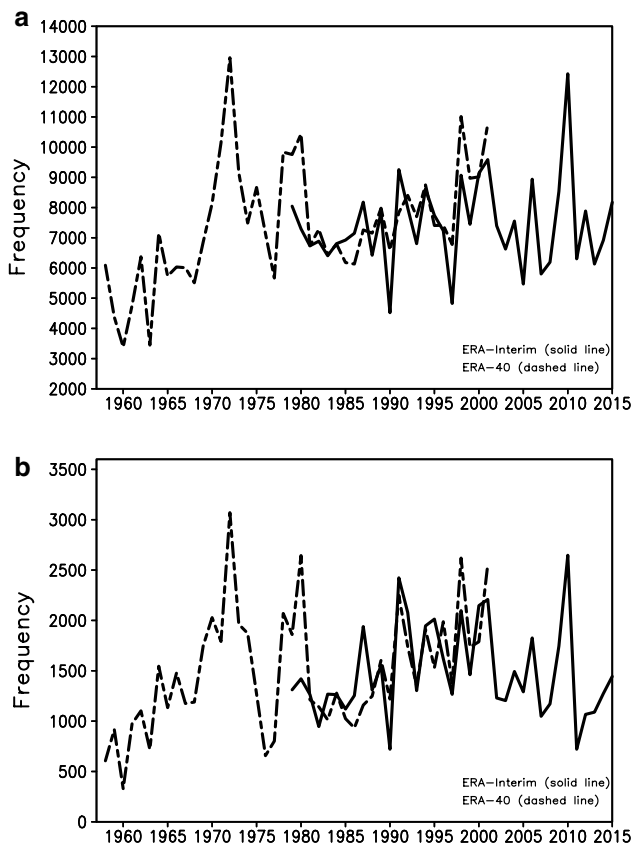
of the total count of extreme precipitation events (*blue*), PC1 (*green*), PC2 (*red*) and PC3 (*yellow*). The inter-annual variations of total count of extreme precipitation events are calculated over the box ( $64^{\circ}$ – $76^{\circ}$ E,  $32^{\circ}$ – $38^{\circ}$ N) in the WH region

Figure 6 shows spatial maps generated by regressing the time series of extreme rainfall index (PC2) on mean winds, rainfall, sea-level pressure, and SST for the period 1958–2001. The rainfall regression map shows positive anomalies over Himalayan foothills, Pakistan, and both northwestern and northeastern India. Negative anomalies are found over Central India and the Western Ghats (Fig. 6a). This pattern is consistent with the spatial map of trend in JJAS rainfall (Fig. 3d), with a high spatial correlation of 0.88 over the Indian subcontinent. Further, the regression map of 700 hPa winds shows westerly and southwesterly anomalies overlying the positive anomaly of rainfall over Pakistan.

Much monsoonal rain occurs over and upstream of the western Ghats and mountains of Burma in association with the low-level southwesterly monsoon flow (Houze et al. 2016). The easterly anomalies over the Bay of Bengal, Indian peninsula and the Arabian Sea indicate a slow-down of the lower-level climatological southwesterly monsoon winds (e.g., Krishnan et al. 2013). In addition, synoptic-scale circulation patterns such as monsoon depressions emanating from the Bay of Bengal (Shukla 1978; Krishnan et al. 2011) mediate the mesoscale and convective-scale manifestations of monsoon rainfall (Houze et al. 2007; Medina et al. 2010). Generally active monsoon spells

(Choudhury and Krishnan, 2011), have a similar mediating effect, possibly because they favor Bay of Bengal depression occurrence. While studies have reported significant decreasing trend in the frequency of monsoon depressions during the recent few decades (e.g. Guhathakurta and Rajeevan 2008; Krishnamurti et al. 2013), further investigations are necessary to fully comprehend the complex pathways through which mesoscale organization of precipitation can be influenced due to weakening of the background climatological and synoptic-scale circulation of the monsoon.

Regression maps of 500 hPa and 200 hPa winds show dominance of sub-tropical westerlies extending across the Arabian region into the Indian subcontinent and further eastward (Fig. 6b–c). The appearance of westerly anomalies at these latitudes reflect an upper-air cyclonic anomaly pattern over the region of northwest India, Pakistan and Afghanistan. Such patterns are reminiscent of “breaks” in the Indian monsoon (e.g. Ramaswamy 1962; Krishnan et al. 1998, 2000, 2009; Vellore et al. 2014). Concurrently, a high-pressure anomaly occurs over central India and the adjoining Bay of Bengal (Fig. 6d). The regression map of SST on the time series of extreme rainfall index shows a warming pattern over the west-central equatorial Indian



**Fig. 5** Time series of yearly total count of extreme upward motions over the WH region ( $64^{\circ}$ – $76^{\circ}$ E,  $32^{\circ}$ – $38^{\circ}$ N). The count is determined using the daily 500 hPa vertical velocity ( $\omega$ ) field for **a** when  $-\omega \geq 95$ th percentile, **b** when  $-\omega \geq 99$ th percentile. The calculation is performed every day of the JJAS monsoon season at all the grid-points in the WH domain during the period (1958–2001) using the ERA-40 reanalysis data (*dashed line*). The solid line is the count of extreme upward motions based on the ERA-interim reanalysis data for the period (1979–2015). A clear positive trend (685 counts per 37 years) during the period (1979–2015) is evident for the 95th percentile threshold, indicative of enhancements in moderate to strong convective motions over the WH region. On the other hand, the rather weak positive trend (60 counts per 37 years) for the 99th percentile threshold suggests lesser enhancements of intense deep convection

Ocean (Fig. 6e). This feature is consistent with recent studies on the relationship between the weakening trend of the Indian monsoon rainfall and the warming of equatorial Indian Ocean SST by  $0.5$ – $1.0$   $^{\circ}$ C during the post-1950s (e.g., Swapna et al. 2014; Roxy et al. 2015).

The strength of the large-scale monsoon circulation may be expressed using the Webster–Yang Index (WYI, see Webster and Yang 1992), which is a measure of the vertical shear of the monsoon circulation, computed as the difference of zonal winds between the lower and upper tropospheric levels (U850–U200). We computed daily time-series of WYI using daily zonal winds from reanalysis

products, covering the period 1951–2007, to identify days having strong monsoon vertical shear (i.e.,  $WYI > 1$  SD) and weak monsoon vertical shear ( $WYI < -1$  SD) respectively. Yearly counts of days having strong and weak monsoon vertical shear are calculated for every JJAS monsoon season. Figure 7a shows the yearly time-series of strong monsoon (blue line) and weak monsoon (red line) days. The days with weak monsoon vertical shear exhibit a significant positive trend, while the opposite is seen for the time-series of days with strong monsoon vertical shear. This information is used to stratify the counts of daily precipitation extremes over the WH region (Fig. 4d, blue line) with respect to days with weak and strong monsoon vertical shear. This is done by binning the counts of daily precipitation extremes in the strong or weak monsoon category depending on whether  $WYI > 1$  or  $< -1$  SD on that particular day. The time-series of daily precipitation extremes for the weak and strong monsoon categories are shown in Fig. 7b. The time-series of frequency of daily precipitation extremes over WH, coincident with weak monsoon category, shows an upward trend. However, the corresponding time-series of daily precipitation extremes for the strong monsoon category does not exhibit a significant trend. Collection of total counts of daily precipitation extremes for different decades (1953–1963, 1964–1974, ..., 1997–2007) for the two categories is shown in Fig. 7c. It is interesting to see that the daily precipitation extremes over the WH in the last two decades were predominantly associated with the weak monsoon category.

The increasing trend of heavy rainfall over the upper Indus basin for the period 1998–2015 is also captured in the TRMM3B42 dataset (Auxiliary Fig. A3). To confirm the robustness of the statistics of daily precipitation extremes over the WH region, we have compared the APHRODITE and TRMM3B42 precipitation datasets for the common period 1998–2007 (see Table 1). Both precipitation datasets have the same horizontal resolution of  $0.25^{\circ} \times 0.25^{\circ}$ . The total number of precipitation events over the WH region ( $64^{\circ}$ E– $76^{\circ}$ E,  $32^{\circ}$ N– $38^{\circ}$ N) exceeding the 99th percentile are found to be 14,014 and 14,046 for the APHRODITE and TRMM3B42 datasets respectively. The count of precipitation extremes over the WH region, based on the APHRODITE dataset, associated with the strong and weak monsoon categories are found to be 1870 (13% of total) and 2500 (18% of total) respectively (Table 1). Likewise the corresponding counts based on the TRMM3B42 dataset are found to be 1287 (9% of total) and 2309 (16% of total) respectively. The above analysis indicates that weak (strong) monsoon circulations, as defined by the WYI dynamical measure, are associated with significantly higher (lower) frequency of daily precipitation extremes over the WH region.



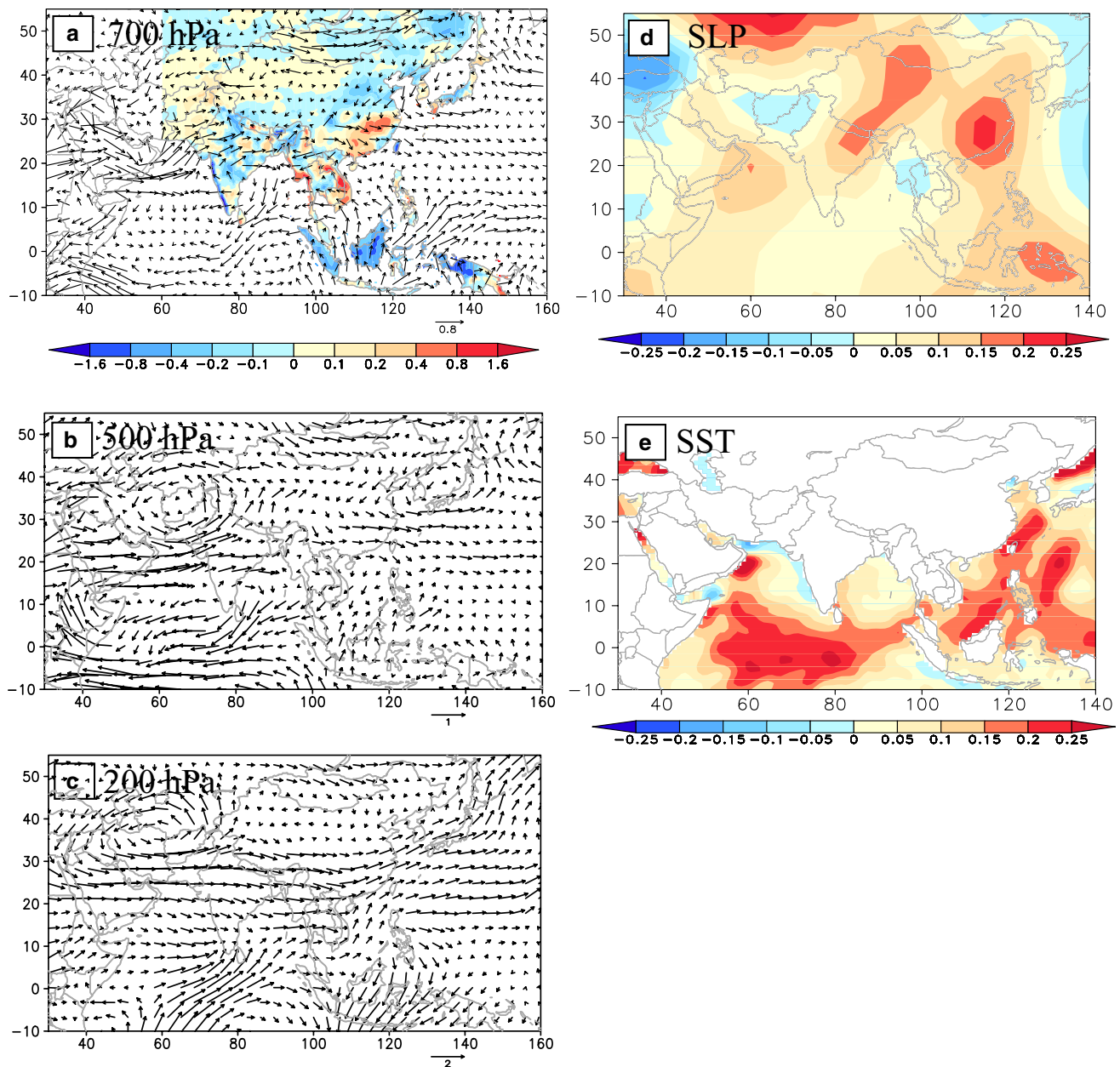


**Fig. 6** **a** Patterns obtained by regressing JJAS rainfall and 700 hPa winds on to the PC2 time-series **b** same as (a) but for 500 hPa winds **c** same as (a) but for 200 hPa winds **d** same as (a) but for sea level pressure **e** same as (a) but for sea surface temperature. The regression analysis is carried out for the period 1958–2001. The obtained

rainfall (unit:  $\text{mm day}^{-1}$ , winds (unit:  $\text{ms}^{-1}$ ), sea level pressure [unit: hPa (SD of PC2) $^{-1}$ ] and sea surface temperature [unit:  $^{\circ}\text{C}$  (SD of PC2) $^{-1}$ ] patterns are based on the APHRODITE, ERA40 reanalysis, HadISLP2 and HadISST data sets respectively

### 3.2 Changes in frequency of extratropical westerly troughs combining with moisture influx from tropics

Here we examine variations in the transient activity of westerly troughs over the region covering the Indus basin and northwest India–Pakistan using daily horizontal winds at 500 hPa from the ERA40 (1958–2002) and ERA Interim

(1979–2013) reanalysis datasets. The transient activity of westerly troughs is measured in terms of relative vorticity computed from the daily wind fields. We counted the occurrences of cyclonic vorticity exceeding 1 SD at each grid point over the domain  $55^{\circ}\text{E}$ – $75^{\circ}\text{E}$ ,  $20^{\circ}\text{N}$ – $55^{\circ}\text{N}$ . Basically, the total count of cyclonic vorticity occurrences for a given JJAS season provides a measure of transient westerly trough activity over that region for that particular year. The

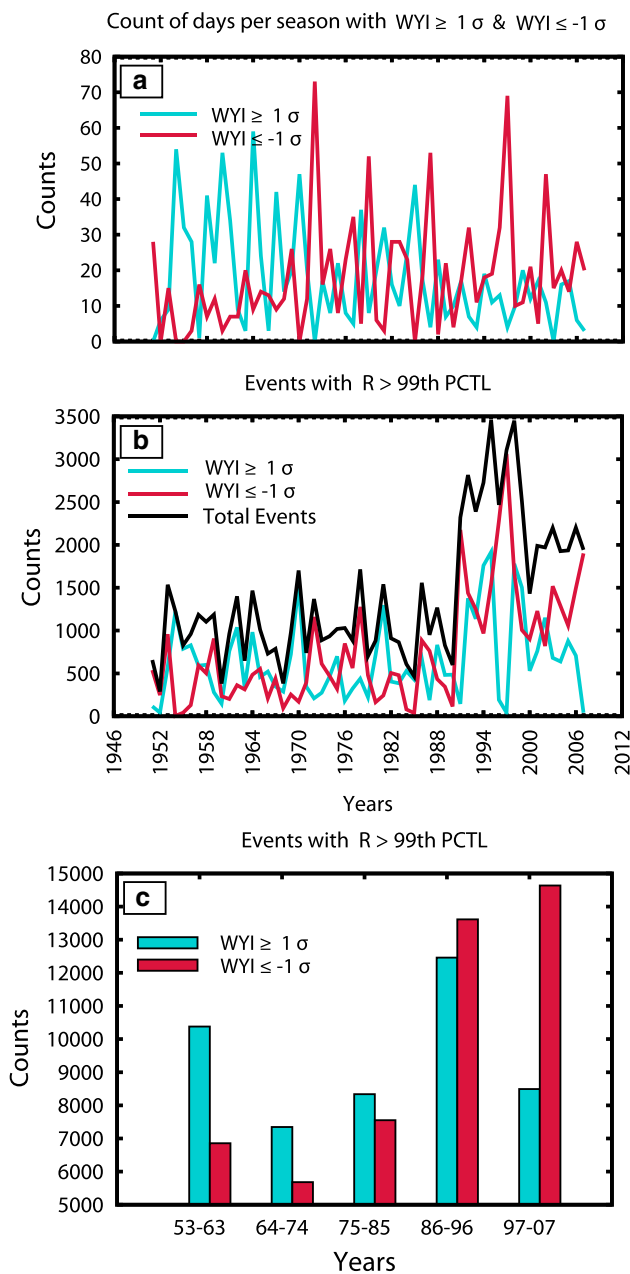


**Fig. 7** Time-series of **a** number of days with strong and weak vertical shear of monsoon based on the WYI criterion. The time-series corresponding to the weak monsoon phase shows a positive trend (15 days per 57 years) which is statistically significant ( $p > 0.05$ ), **b** Total number of heavy rainfall events (rainfall  $\geq$  99th percentile) over the box ( $64^{\circ}\text{E}$ – $76^{\circ}\text{E}$ ,  $32^{\circ}\text{N}$ – $38^{\circ}\text{N}$ ) shown by black line, the count of heavy rainfall events coinciding with strong (blue line) and weak (red line) phases of the monsoon as defined by the WYI criterion, **c** Cumulative counts of heavy rainfall coinciding with strong and weak monsoons for the decades (1953–1963), (1964–1974), (1975–1985), (1986–1996) and (1997–2007) over the same box as in (b)

total counts are determined for the entire JJAS season and this analysis is repeated for all the years. By so doing, we obtain yearly time-series of the transient westerly trough

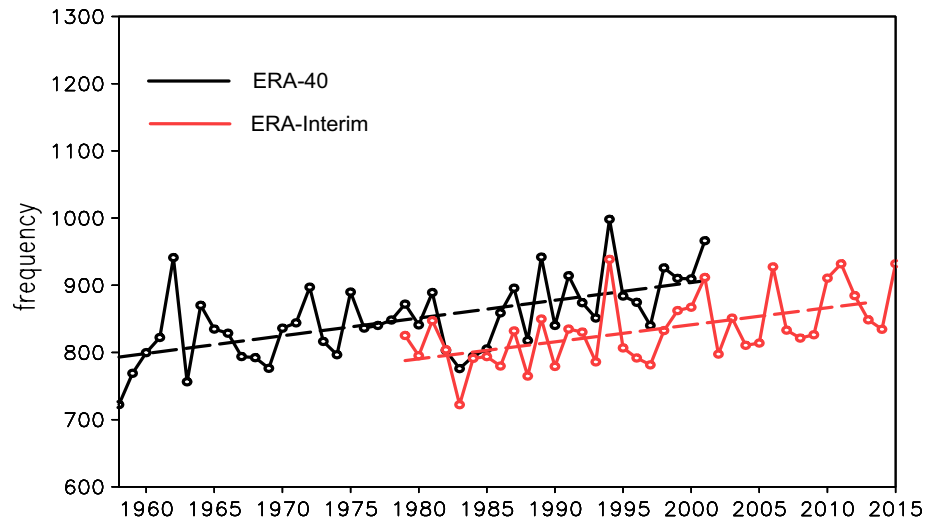
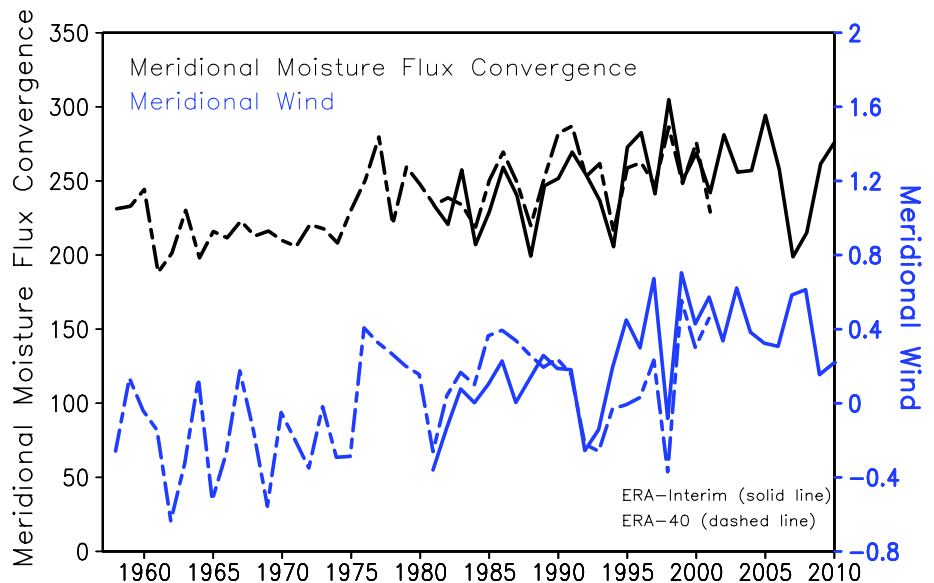
activity over the WH region (Fig. 8). The frequency count of westerly trough activity over the WH has a significant increasing trend in both the reanalysis datasets during the common period (1979–2002). This increasing trend in the cyclonic vorticity occurrences over the WH region is indicative of the increasing propensity of transient westerly troughs that can allow triggering of deep convection in the presence of moisture supply particularly due to southerly flow from the Arabian Sea (see Houze et al. 2007; Medina et al. 2010). Figure 9 shows the time-series of vertically integrated (surface to 300 hPa) moisture convergence associated with the meridional winds  $-\frac{\partial(vq)}{\partial y}$  (black line), averaged over the domain ( $60^{\circ}\text{E}$ – $73^{\circ}\text{E}$ ,  $15^{\circ}\text{N}$ – $30^{\circ}\text{N}$ ) covering the northern Arabian Sea and adjoining areas of northwest India and Pakistan, for the ERA-40 and ERA-Interim reanalyses. A clear increasing trend (significant at 0.01 level) in the moisture convergence associated with meridional winds is evident in both the reanalysis datasets for the common period (1981–2002). The time-series of meridional component of wind averaged over the same region shows a significant increasing trend (blue line, Fig. 9). The increasing trend of southerly winds over the northern Arabian Sea has also been reported by Sandeep and Ajayamohan (2015). Moisture transport from the Arabian Sea into WH is crucial in supporting deep convection over the subtropical areas around northwest India and Pakistan (see Houze et al. 2007; Medina et al. 2010; Priya et al. 2015).

Vellore et al. (2015) have shown that major precipitation events in the Himalayan region can occur when the moisture transport associated with a monsoon low combines favorably with an upper-level westerly trough extending southward into the Himalayan region. The analyses in the present paper indicate that both upper-level westerly troughs and large moisture transport from the south are increasing over time. However, there is no assurance that these two factors will coincide and reinforce each other to produce a major rain event. Studies showed that the Uttarakhand flood of 2013 occurred when such a coincidence of an upper-level westerly trough and monsoon low occurred and formed a moisture transport toward the Himalayan escarpment (Vellore et al. 2015; Krishnamurti et al. 2016). Houze et al. (2016) showed further that the clouds producing the large rainfall in that case were due to a synoptic-scale lifting associated with the trough combined with orographic lifting of the moisture flux. Convective overturning played a minor role.

For a major rain event to occur, the necessary moisture flux need not combine with a trough of midlatitude origin. Houze et al. (2011) and Rasmussen et al. (2015) have shown how a westward extending monsoon low combined with a strong ridge over the Tibetan Plateau to provide the moisture flux in several of the most extreme rain events of recent years. Thus, there are at least two major ways that a

**Table 1** Total count of heavy rainfall occurrences over the box (64°E–76°E, 32°N–38°N) from APHRODITE and TRMM3B42 datasets for the common period 1998–2007 for strong and weak monsoon days based on  $WYI \geq 1$  and  $WYI \leq -1$  SD respectively

Datasets	APHRODITE			TRMM3B42		
	Total	Strong	Weak	Total	Strong	Weak
Count of heavy rainfall occurrences	14,014	1870 (13%)	2500 (18%)	14,046	1287 (9%)	2309 (16%)

**Fig. 8** Time series of frequency of 500 hPa relative vorticity exceeding 1 SD for ERA40 (black) and ERA Interim (red). The frequency is computed using relative-vorticity ( $s^{-1}$ ) for the region (55°–75°E, 20°–55°N)**Fig. 9** Time series of vertically integrated (surface to 300 hPa) moisture flux convergence (unit:  $kg\ ms^{-1}$ ) across the lateral boundary of WH (60°–73°E, 15°–30°N) region during JJAS season (black) and the meridional component of wind ( $ms^{-1}$ ) averaged over the same domain (blue). ERA 40 (dotted) and ERA Interim (solid) datasets are used for the periods 1958–2001 and 1981–2010 respectively

strong synoptic-scale moisture flux can produce major rain events that can sometimes lead to flooding over the Himalayas: either a westward extending monsoon low combines with a ridge over the Tibetan Plateau or with a westerly trough extending southward into the Himalayan region.

The present study shows that both westerly troughs extending into the region and poleward moisture fluxes toward the Himalayas are increasing. It may be conjectured

from these findings that the probability of the westerly-trough type of heavy rain event over the Himalayas is therefore likely increasing. The common denominator of the storms producing major rain events over the Himalayas is the strong large-scale moisture flux. The predictability of such storms (Webster et al. 2010, 2011; Joseph et al. 2014; Rasmussen et al. 2015) is likely a result of the accurate prediction of the large-scale moisture flux by global models.



The likelihood of extreme precipitation alone, however, is not sufficient when considering potential flooding. Whether or not the moisture flux is combined with a trough extending southward from the extratropics or with a ridge over the Tibetan Plateau is relevant to whether the storms are of an intense convective nature or of a more general ascent in which convection plays a minor role. Which type of clouds produce the precipitation is in turn highly relevant to the hydrologic response to the storm; e.g. whether a flash flood or a slow-rising flood is more likely.

#### 4 Concluding remarks

This study is an investigation to understand the recent increasing trend of heavy rain occurrence over the semi-arid to arid mountainous regions in the western flank of the South Asian monsoon system. A positive trend of heavy rain occurrence is seen primarily over the upper Indus basin while the trend is opposite in the lower eastern Indus basin and adjoining Indian landmass. The spatially non-homogeneous pattern of trends in daily precipitation extremes is captured by the second EOF/PC component of the frequency of heavy rainfall. Using TRMM Precipitation Radar observations, Houze et al. (2007, 2016) reported that extreme forms of radar echo over the northwestern regions of the Himalayas during the summer monsoon tend to take the form of deep convective cores, and that mesoscale convection (intense convective systems of large horizontal dimension) occurs infrequently compared to other regions of the Himalayan domain. Storms producing flooding in Pakistan and western India, however, are anomalous in that they are of mesoscale dimension and have associated stratiform precipitation (Rasmussen et al. 2015). The EOF2 spatial pattern associated with positive loading over the upper Indus basin suggests that such mesoscale enhancements of convection are occurring more frequently in the upper Indus basin. At the same time, a significant decreasing trend in the overall seasonal summer monsoon precipitation over India and a weakening trend of the monsoon large-scale circulation is evident in our analysis of the post-1950s.

We infer from our analyses that changes in background flow climatology have likely facilitated enhanced activity of cyclonic troughs over the WH region and a significant enhancement of moisture convergence over the WH region associated with stronger southerly flows from the Arabian Sea during the recent decades. These two results suggest an increasing probability of the type of extreme precipitation event that results from the combination of large-scale moisture flux (associated with a westward extended monsoonal trough) and a southward protruding westerly trough. While the present study raises the role of possible

linkage between changes in background climatology and deep convective activity over the WH region, the occurrence of heavy rain events on smaller scales needs further investigations to adequately comprehend the detailed pathways that account for processes occurring on synoptic, meso-, and convective scales and the associated hydrologic response.

**Acknowledgements** Authors thank IITM for extending all support for this research work. We are grateful to the two anonymous reviewer for suggesting critical value additions to the manuscript. We also thankfully acknowledge scientific discussions and useful suggestions provided by Dr. Ramesh Vellore. IITM is supported by the Ministry of Earth Sciences, Government of India, New Delhi. RAH is supported by National Science Foundation Grant AGS-1503155 and the Pacific Northwest National Laboratory under Task Order 292896 (WAC-CEM) of Master Agreement 243766.

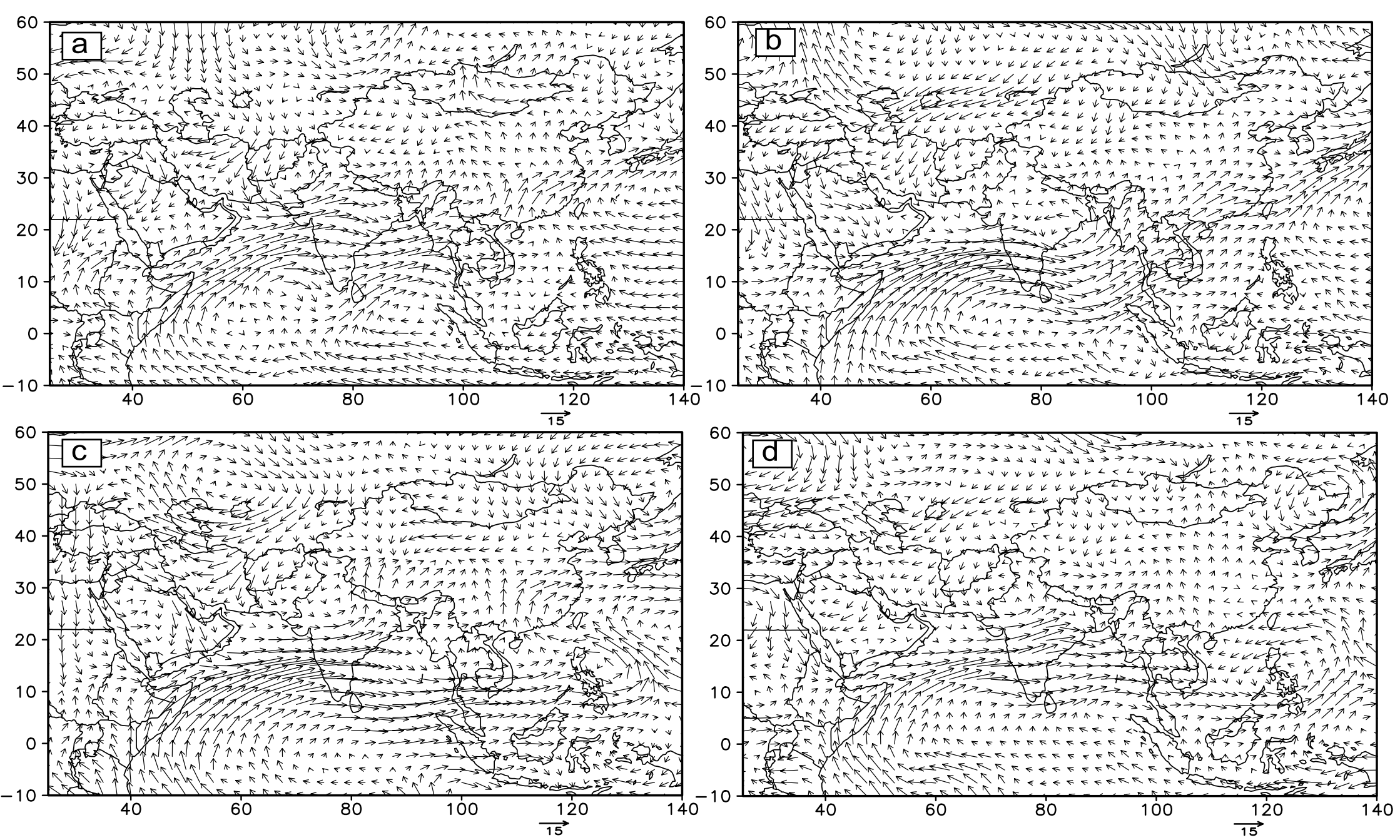
#### References

- Abish B, Joseph PV, Johannessen OM (2013) Weakening trend of the tropical easterly jet stream of the boreal summer monsoon season 1950–2009. *J Clim* 26(23):9408–9414. doi:[10.1175/JCLI-D-13-00440.1](https://doi.org/10.1175/JCLI-D-13-00440.1)
- Allan R, Ansell T (2006) A new globally complete monthly historical gridded mean sea level pressure dataset (HadSLP2): 1850–2004. *J Clim* 19(22):5816–5842
- Arnell NW (2003) Effects of IPCC SRES emissions scenarios on river runoff: a global perspective. *Hydrol Earth Syst Sci* 7(5):619–641. doi:[10.5194/hess-7-619-2003](https://doi.org/10.5194/hess-7-619-2003)
- Barbosa SM, Andersen OB (2009) Trend patterns in global sea surface temperature. *Int J Climatol* 29(14):2049–2055. doi:[10.1002/joc.1855](https://doi.org/10.1002/joc.1855)
- Bolch T, Kulkarni A, Kaab A, Huggel C, Paul F, Cogley JG, Frey H, Kargel JS, Fujita K, Scheel M, Bajracharya S, Stoffel M (2012) The state and fate of Himalayan glaciers. *Science* 336(6079):310–314
- Bookhagen B, Burbank DW (2010) Toward a complete Himalayan hydrological budget: spatio-temporal distribution of snowmelt and rainfall and their impact on river discharge. *J Geophys Res* 115:F03019. doi:[10.1029/2009JF001426](https://doi.org/10.1029/2009JF001426)
- Choudhury AD, Krishnan R (2011) Dynamical response of the South Asian monsoon trough to latent heating from stratiform and convective precipitation. *J Atmos Sci* 68(6):1347–1363. doi:[10.1175/2011JAS3705.1](https://doi.org/10.1175/2011JAS3705.1)
- Compo GP, Sardeshmukh PD (2010) Removing ENSO-related variations from the climate record. *J Clim* 23(8):1957–1978. doi:[10.1175/2009JCLI2735.1](https://doi.org/10.1175/2009JCLI2735.1)
- Danielson JJ, Gesch DB (2011) Global multi-resolution terrain elevation data 2010 (GMTED2010). U.S. Geological Survey Open-File Report 2011–1073:26
- Ding Q, Wang B (2005) Circumglobal Teleconnection in the Northern Hemisphere summer. *J Clim* 18(17):3483–3505. doi:[10.1175/JCLI3473.1](https://doi.org/10.1175/JCLI3473.1)
- Ding Q, Wang B (2007) Intraseasonal teleconnection between the summer Eurasian wave train and the Indian Monsoon. *J Clim* 20:3751–3767. doi:[10.1175/JCLI4221.1](https://doi.org/10.1175/JCLI4221.1)
- Dobhal DP, Gupta AK, Mehta M, Khandelwal DD (2013) Kedarnath disaster: facts and plausible causes. *Curr Sci* 105(2):171–174
- Gardelle J, Berthier E, Arnaud Y (2012) Slight mass gain of Karakoram glaciers in the early twenty-first century. *Nat Geosci*. doi:[10.1038/NGEO1450](https://doi.org/10.1038/NGEO1450)

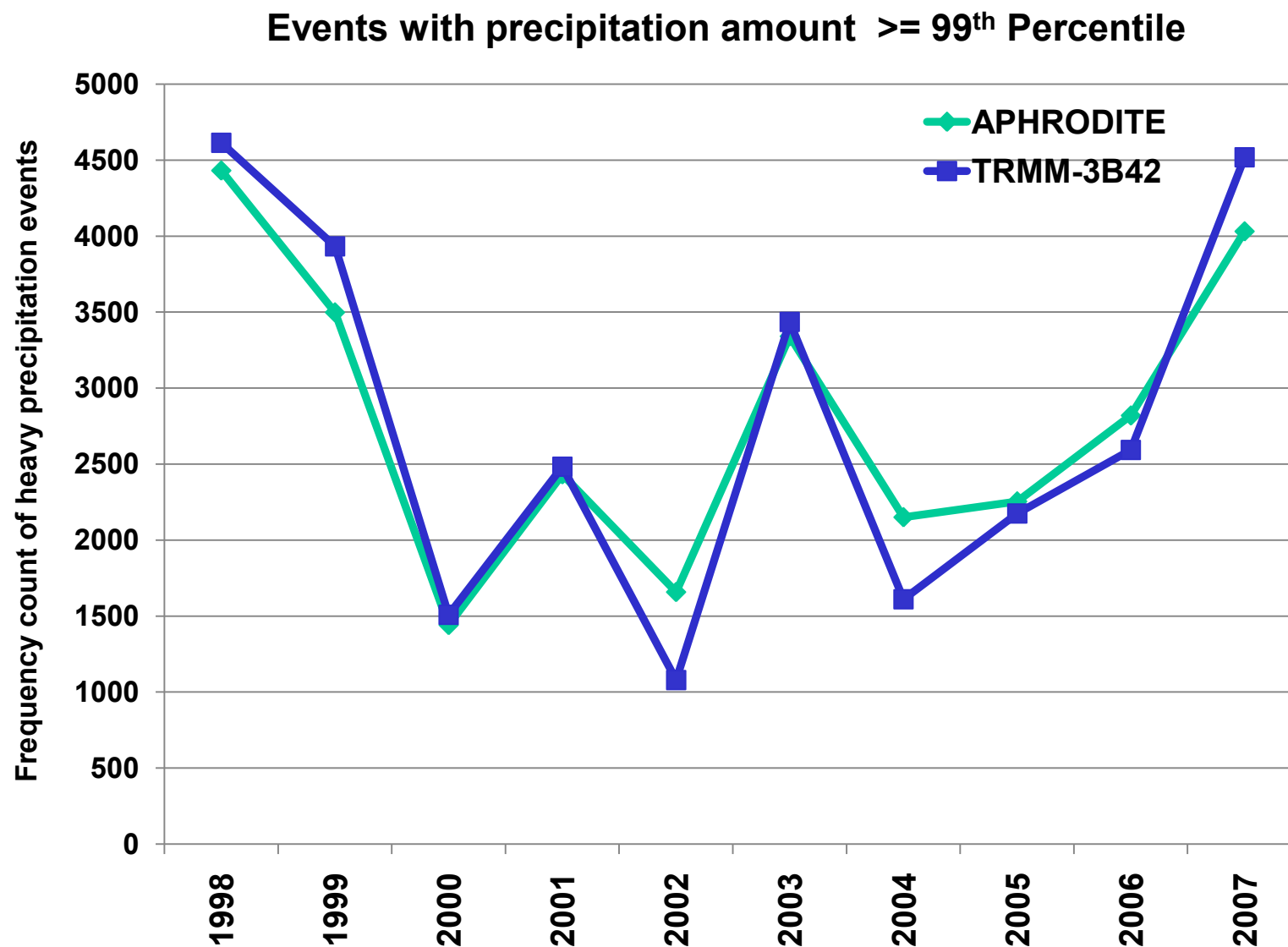
- Ghosh S, Das D, Kao S, Ganguly AR (2011) Lack of uniform trends but increasing spatial variability in observed Indian rainfall extremes. *Nat Clim Chang* 2(2):86–91. doi:[10.1038/nclimate1327](https://doi.org/10.1038/nclimate1327)
- Giorgi F, Hurrell W, Mainucci MR (1997) Elevation dependency of the surface climate change signal: a model study. *J Clim* 10(2):288–296. doi:[10.1175/1520-0442\(1997\)010<0288:EDOTSC>2.0.CO;2](https://doi.org/10.1175/1520-0442(1997)010<0288:EDOTSC>2.0.CO;2)
- Guhathakurta P, Rajeevan M (2008) Trends in the rainfall pattern over India. *Int J Climatol* 28(11):1453–1469. doi:[10.1002/joc](https://doi.org/10.1002/joc)
- Hasson S, Lucarini V, Khan MR, Petitta M, Bolch T, Gioli G (2014) Early 21st century snow cover state over the western river basins of the Indus River system. *Hydrol Earth Sys Sci* 18:4077–4100. doi:[10.5194/hess1840772014](https://doi.org/10.5194/hess1840772014)
- Hasson S, Lucarini V, Pascale S (2013) Hydrological cycle over South and Southeast Asian river basins as simulated by PCMDI/CMIP3 experiments. *Earth Sys Dyn* 4(2):199–217. doi:[10.5194/esd-4-199-2013](https://doi.org/10.5194/esd-4-199-2013)
- Hasson S, Pascale S, Lucarini V, Böhner J (2016) Seasonal cycle of precipitation over major river basins in South and Southeast Asia: a review of the CMIP5 climate models data for present climate and future climate projections. *Atmos Res* 180:42–63. doi:[10.1016/j.atmosres.2016.05.008](https://doi.org/10.1016/j.atmosres.2016.05.008)
- Hong CC, Hsu HH, Lin NH, Chiu H (2011) Roles of European blocking and tropical extratropical interaction in the 2010 Pakistan flooding. *Geophys Res Lett* 38(13):1–6. doi:[10.1029/2011GL047583](https://doi.org/10.1029/2011GL047583)
- Houze RA, Wilton D, Smull B (2007) Monsoon convection in the Himalayan region as seen by the TRMM Precipitation Radar. *Q J R Meteorol Soc* 133(627):1389–1411. doi:[10.1002/qj.106](https://doi.org/10.1002/qj.106)
- Houze RA, Rasmussen KL, Medina S, Brodzik SR, Romatschke U (2011) Anomalous atmospheric events leading to the summer 2010 floods in Pakistan. *Bull Am Meteorol Soc* 92(3):291–298. doi:[10.1175/2010BAMS3173.1](https://doi.org/10.1175/2010BAMS3173.1)
- Houze, RA, Rasmussen KL, McMurdie L, Chaplin MM, Kumar A (2016) Synoptic and mesoscale aspects of the June 2013 flooding in Uttarakhand, India. *Mon Wea Rev* (submitted)
- Hsiung J, Newell RE (1983) The principal non seasonal modes of variation of global sea surface temperature. *J Phys Oceanogr* 13(10):1957–1967. doi:[10.1175/1520-0485\(1983\)013<1957:TPNMOV>2.0.CO;2](https://doi.org/10.1175/1520-0485(1983)013<1957:TPNMOV>2.0.CO;2)
- Huffman GJ, Adler RF, Bolvin DT, Gu G, Nelkin EJ, Bowman KP, Hong Y, Stocker EF, Wolff DB (2007) The TRMM multi-satellite precipitation analysis: quasi-global, multi-year, combined-sensor precipitation estimates at fine scale. *J Hydrometeorol* 8(1):38–55. doi:[10.1175/JHM560.1](https://doi.org/10.1175/JHM560.1)
- Hussain MS, Lee S (2013) The regional and the seasonal variability of extreme precipitation trends in Pakistan. *Asia Pac J Atmos Sci* 49(4):421–441. doi:[10.1007/s13143-013-0039-5](https://doi.org/10.1007/s13143-013-0039-5)
- Immerzeel WW, van Beek LPH, Bierkens MFP (2010) Climate change will affect the Asian water towers. *Science* 328:1382–1385
- Joseph S, Sahai AK, Sharmila S, Abhilash S, Borah N, Chattopadhyay R, Pillai PA, Rajeevan M, Kumar A (2014) North Indian heavy rainfall event during June 2013: diagnostics and extended range prediction. *Clim Dyn*. doi:[10.1007/s00382-014-2291.5](https://doi.org/10.1007/s00382-014-2291.5)
- Joseph PV, Simon A (2005) Weakening trend of the southwest monsoon current through peninsular India from 1950 to the present. *Curr Sci* 89(4):687–694
- Kapnick SB, Delworth TL, Ashfaq M, Malyshev S, Milly PCD (2014) Snowfall less sensitive to warming in Karakoram than in Himalayas due to a unique seasonal cycle. *Nat Geosci* 7:834–840
- Kistler R et al (2001) The NCEP-NCAR 50-year reanalysis: monthly means CD-ROM and documentation. *Bull Amer Meteorol Soc* 82(2):247–267. doi:[10.1175/1520-0477\(2001\)082<0247:TNNYRM>2.3.CO;2](https://doi.org/10.1175/1520-0477(2001)082<0247:TNNYRM>2.3.CO;2)
- Klein Tank AMG et al (2006) Changes in daily temperature and precipitation extremes in central and south Asia. *J Geophys Res* 111(D16). doi:[10.1029/2005JD006316](https://doi.org/10.1029/2005JD006316)
- Krishnamurthy CKB, Lall U, Kwon HH (2009) Changing frequency and intensity of rainfall extremes over India from 1951 to 2003. *J Clim* 22(18):4737–4746. doi:[10.1029/2005JD006316](https://doi.org/10.1029/2005JD006316)
- Krishnamurti TN, Kumar V, Simon A, Thomas A, Bhardwaj A, Das S, Senroy S, Roy Bhowmik SK (2016) March of buoyancy elements during extreme rainfall over India. *Clim Dyn*. doi:[10.1007/s00382-016-3183-7](https://doi.org/10.1007/s00382-016-3183-7)
- Krishnamurti TN, Martin A, Krishnamurti R, Simon A, Thomas A, Kumar V (2013) Impacts of enhanced CCN on the organization of convection and recent reduced counts of monsoon depressions. *Clim Dyn* 41(1):117–134. doi:[10.1007/s00382-012-1638-z](https://doi.org/10.1007/s00382-012-1638-z)
- Krishnan R, Ayantika DC, Kumar V, Pokrel S (2011) The long-lived monsoon depressions of 2006 and their linkage with the Indian Ocean Dipole. *Int J Climatol* 30(9):1334–1352. doi:[10.1002/joc.2156](https://doi.org/10.1002/joc.2156)
- Krishnan R, Kumar V, Sugi M, Yoshimura J (2009) Internal feedbacks from monsoon–midlatitude interactions during droughts in the Indian summer monsoon. *J Atmos Sci* 66(3):553–578. doi:[10.1175/2008JAS2723.1](https://doi.org/10.1175/2008JAS2723.1)
- Krishnan R, Sabin TP, Ayantika DC, Kitoh A, Sugi M, Murakami H, Turner AG, Slingo JM, Rajendran K (2013) Will the South Asian monsoon overturning circulation stabilize any further? *Clim Dyn* 40(1):187–211. doi:[10.1007/s00382-012-1317-0](https://doi.org/10.1007/s00382-012-1317-0)
- Krishnan R, Sabin TP, Vellore R, Mujumdar M, Sanjay J, Goswami BN, Hourdin E, Dufresne J-L, Terray P (2015) Deciphering the desiccation trend of the south Asian monsoon hydroclimate in a warming world. *Clim Dyn* 47(3):1007–1027. doi:[10.1007/s00382-015-2886-5](https://doi.org/10.1007/s00382-015-2886-5)
- Krishnan R, Sugi M (2001) Baiu rainfall variability and associated monsoon teleconnections. *J Meteorol Soc Jpn* 79:851–860
- Krishnan R, Venkatesan C, Keshavamurthy RN (1998) Dynamics of upper tropospheric stationary wave anomalies induced by ENSO during the northern summer—a GCM study. *Proc Indian Acad Sci EPS (Present J Earth Syst Sci)* 107:65–90
- Krishnan R, Zhang C, Sugi M (2000) Dynamics of breaks in the Indian summer monsoon. *J Atmos Sci* 57:1354–1372
- Kumar A, Houze RA Jr, Rasmussen KL, Peters-Lidard C (2014) Simulation of a flash flooding storm at the steep edge of the Himalayas. *J Hydrometeorol* 15(1):212–228. doi:[10.1175/JHM-D-12-0155.1](https://doi.org/10.1175/JHM-D-12-0155.1)
- Latif M, Syed FS, Hannachi A (2016) Rainfall trends in the South Asian summer monsoon and its related large-scale dynamics with focus over Pakistan. *Clim Dyn*. doi:[10.1007/s00382-016-3284-3](https://doi.org/10.1007/s00382-016-3284-3)
- Lau WK, Kim KM (2012) The 2010 Pakistan flood and Russian heat wave: teleconnection of hydrometeorological extremes. *J Hydrometeorol* 13(1):392–403. doi:[10.1175/JHM-D-11-016.1](https://doi.org/10.1175/JHM-D-11-016.1)
- Lotus S (2015) Heavy rainfall over Jammu & Kashmir during 3–6 September, 2014 leading to flooding condition. *Monsoon 2014: a report (ESSO/IMD/SYNOPTIC MET/01(2015)/17)*. India Meteorological Department, National Climate Center, Pune, India
- Malik N, Bookhagen B, Marwan N, Kurths J (2012) Analysis of spatial and temporal extreme monsoonal rainfall over South Asia using complex networks. *Clim Dyn* 39(3):971–987. doi:[10.1007/s00382-011-1156-4](https://doi.org/10.1007/s00382-011-1156-4)
- Malik N, Bookhagen B, Mucha PJ (2016) Spatiotemporal patterns and trends of Indian monsoonal rainfall extremes. *Geophys Res Lett* 43(4):1710–1717. doi:[10.1002/2016GL067841](https://doi.org/10.1002/2016GL067841)
- Martius O, Sodemann H, Joos H, Pfahl S, Winschall A, Croci-Maspoli M, Graf M, Madonna E, Mueller B, Schemm S, Sedláček J, Wernli H (2013) The role of upper-level dynamics and surface processes for the Pakistan flood of July 2010. *Q J R Meteorol Soc* 139(676):1780–1797. doi:[10.1002/qj.2082](https://doi.org/10.1002/qj.2082)

- Medina S, Houze RA, Kumar A, Niyogi D (2010) Summer monsoon convection in the Himalayan region: terrain and land cover effects. *Q J R Meteorol Soc* 136(648):593–616. doi:[10.1002/qj.601](https://doi.org/10.1002/qj.601)
- Messerli B, Viviroli D, Weingartner R (2004) Mountains of the world: vulnerable water towers for the 21st century. *Ambio* 13:29–34
- Mishra V, Smoliak BV, Lettenmaier DP, Wallace JM (2012) A prominent pattern of year-to-year variability in Indian Summer Monsoon Rainfall. *Proc Natl Acad Sci* 109(19):7213–7217. doi:[10.1073/pnas.1119150109](https://doi.org/10.1073/pnas.1119150109)
- Mujumdar M, Preethi B, Sabin TP, Ashok K, Saeed S, Pai DS, Krishnan R (2012) The Asian summer monsoon response to the La Nina event of 2010. *Meteorol Appl* 19(2):216–225. doi:[10.1002/met.1301](https://doi.org/10.1002/met.1301)
- Nijssen B, Lettenmaier DP, Liang X, Wetzel SW, Wood EF (1997) Streamflow simulation for continental scale river basins. *Water Resour Res* 33(4):711–724. doi:[10.1029/96WR03517](https://doi.org/10.1029/96WR03517)
- Priya P, Mujumdar M, Sabin TP, Terray P, Krishnan R (2015) Impacts of Indo-Pacific sea surface temperature anomalies on the summer monsoon circulation and heavy precipitation over northwest India–Pakistan region during 2010. *J Clim* 28(9):3714–3730. doi:[10.1175/JCLI-D-14-00595.1](https://doi.org/10.1175/JCLI-D-14-00595.1)
- Ramaswamy C (1962) Breaks in the Indian summer monsoon as a phenomenon of interaction between the easterly and the sub-tropical westerly jet streams. *Tellus* 14(3):337–349. doi:[10.1111/j.2153-3490.1962.tb01346.x](https://doi.org/10.1111/j.2153-3490.1962.tb01346.x)
- Rangwala I, Miller JR (2012) Climate change in mountains: a review of elevation-dependent warming and its possible causes. *Clim Chang* 114(3):527–547. doi:[10.1007/s10584-012-0419-3](https://doi.org/10.1007/s10584-012-0419-3)
- Rangwala I, Sinsky E, Miller JR (2013) Amplified warming projections for high altitude regions of the northern hemisphere mid-latitudes from CMIP5 models. *Environ Res Lett* 8(2). doi:[10.1088/1748-9326/8/2/024040](https://doi.org/10.1088/1748-9326/8/2/024040)
- Rasmussen KL, Hill AJ, Toma VE, Zuluaga MD, Webster PJ, Houze RA (2015) Multiscale analysis of three consecutive years of anomalous flooding in Pakistan. *Q J R Meteorol Soc* 141(689):1259–1276. doi:[10.1002/qj.2433](https://doi.org/10.1002/qj.2433)
- Rasmussen KL, Houze RA Jr (2012) A flash flooding storm at the steep edge of high terrain: disaster in the Himalayas. *Bull Am Meteorol Soc* 93(11):1713–1724. doi:[10.1175/BAMS-D-11-00236.1](https://doi.org/10.1175/BAMS-D-11-00236.1)
- Rayner NA, Parker DE, Horton EB, Folland CK, Alexander LV, Rowell DP, Kent EC, Kaplan A (2003) Global analyses of sea surface temperature, sea ice, and night marine air temperature since the late nineteenth century. *J Geophys Res* 108(D14):4407. doi:[10.1029/2002JD002670](https://doi.org/10.1029/2002JD002670)
- Roxy MK, Ritika K, Terray P, Murtugudde R, Ashok K, Goswami BN (2015) Drying of Indian subcontinent by rapid Indian Ocean warming and a weakening land-sea thermal gradient. *Nat Commun* 6. doi:[10.1038/ncomms8423](https://doi.org/10.1038/ncomms8423)
- Saeed S, Müller WA, Hagemann S, Jacob D (2011) Circumglobal wave train and the summer monsoon over northwestern India and Pakistan: the explicit role of the surface heat low. *Clim Dyn* 37(5):1045–1060. doi:[10.1007/s00382-010-0888-x](https://doi.org/10.1007/s00382-010-0888-x)
- Salma S, Rehman S, Shah MA (2012) Rainfall trends in different climate zones of Pakistan. *Pak J Meteorol* 9(17):37–47
- Sandeep S, Ajayamohan RS (2015) Poleward shift in Indian summer monsoon low level jetstream under global warming. *Clim Dyn* 45(1):337–351
- Santer BD, Boyle JS, Hnilo JJ, Taylor KE, Wigley TML, Nychka D, Parker DE, Taylor KE (2000) Statistical significance of trends and trend differences in layer-average atmospheric temperature time series. *J Geophys Res* 105(D6):7337–7356. doi:[10.1029/1999JD901105](https://doi.org/10.1029/1999JD901105)
- Sathiyamoorthy V (2005) Large scale reduction in the size of the Tropical Easterly Jet. *Geophys Res Lett* 32(14). doi:[10.1029/2005GL022956](https://doi.org/10.1029/2005GL022956)
- Sawyer JS (1947) The structure of the intertropical front over N.W. India during the S.W. Monsoon. *Q J R Meteorol Soc* 73(317–318):346–369. doi:[10.1002/qj.49707331709](https://doi.org/10.1002/qj.49707331709)
- Shukla J (1978) CISK-barotropic-baroclinic instability and the growth of monsoon depressions. *J Atmos Sci* 35(3):495–508
- Singh D, Tsiang M, Rajaratnam B, Diffenbaugh NS (2014) Observed changes in extreme wet and dry spells during the South Asian summer monsoon season. *Nat Clim Chang* 4(6):456–461. doi:[10.1038/nclimate2208](https://doi.org/10.1038/nclimate2208)
- Srivastava AK, Dutta S, Kshirsagar SR, Srivastava K (2014) Has influence of extratropical waves in modulating Indian summer monsoon rainfall (ISMR) increased? *J Earth Syst Sci* 123(3):445–456. doi:[10.1007/s12040-014-0413-4](https://doi.org/10.1007/s12040-014-0413-4)
- Sugiyama M, Shiogama H, Emori S (2010) Precipitation extreme changes exceeding moisture content increases in MIROC and IPCC climate models. *Proc Natl Acad Sci USA* 107(2):71–75. doi:[10.1073/pnas.0903186107](https://doi.org/10.1073/pnas.0903186107)
- Swapna P, Krishnan R, Wallace JM (2014) Indian Ocean and monsoon coupled interactions in a warming environment. *Clim Dyn* 42(9):2439–2454. doi:[10.1007/s00382-013-1787-8](https://doi.org/10.1007/s00382-013-1787-8)
- Uppala S, Dee D, Kobayashi S, Berrisford P, Simmons A (2008) Towards a climate data assimilation system: status update of ERA-interim. *ECMWF Newsl* 115:12–18
- Uppala SM, Kållberg PW, Simmons AJ, Andrae U, da Costa Bechtold V, Fiorino M, Gibson JK, Haseler J, Hernandez A, Kelly GA, Li X, Onogi K, Saarinen S, Sokka N, Allan RP, Andersson E, Arpe K, Balmaseda MA, Beljaars ACM, van de Berg L, Bidlot J, Bormann N, Caires S, Dethof A, Dragosavac M, Fisher M, Fuentes M, Hagemann S, Hólm E, Hoskins BJ, Isaksen I, Janssen PAEM, McNally AP, Mahfouf J-F, Jenne R, Morcrette J-J, Rayner NA, Saunders RW, Simon P, Sterl A, Trenberth KE, Untch A, Vasiljevic D, Viterbo P, Woollen J (2005) The ERA-40 reanalysis. *Q J R Meteorol Soc* 131(612):2961–3012. doi:[10.1256/qj.04.176](https://doi.org/10.1256/qj.04.176)
- Vellore RK, Kaplan ML, Krishnan R, Lewis JM, Sabade S, Deshpande N, Madhura RK, Ramarao MVS (2015) Monsoon-extra-tropical circulation interactions in Himalayan extreme rainfall. *Clim Dyn* 46(11):3517–3546. doi:[10.1007/s00382-015-2784-x](https://doi.org/10.1007/s00382-015-2784-x)
- Vellore R, Krishnan R, Pendharkar J, Choudhury AD, Sabin TP (2014) On anomalous precipitation enhancement over the Himalayan foothills during monsoon breaks. *Clim Dyn* 43(7):2009–2031. doi:[10.1007/s00382-013-2024-1](https://doi.org/10.1007/s00382-013-2024-1)
- Wang SY, Davies RE, Huang WR, Gillies RR (2011) Pakistan's two stage monsoon and links with the recent climate change. *J Geophys Res* 116(D16):1–15. doi:[10.1029/2011JD015760](https://doi.org/10.1029/2011JD015760)
- Webster PJ, Jian J, Hopson TM, Hoyos CD, Agudelo PA, Chang H-R, Curry JA, Grossman RL, Palmer TN, Subbiah AR (2010) Extended range probabilistic forecasts of Ganges and Brahmaputra floods in Bangladesh. *Bull Am Meteorol Soc* 91(11):1493–1514. doi:[10.1175/2010BAMS2911.1](https://doi.org/10.1175/2010BAMS2911.1)
- Webster PJ, Toma VE, Kim H-M (2011) Were the 2010 Pakistan floods predictable? *Geophys Res Lett* 38(4). doi:[10.1029/2010GL046346](https://doi.org/10.1029/2010GL046346)
- Webster PJ, Yang S (1992) Monsoon and ENSO: selectively interactive systems. *Q J R Meteorol Soc* 118(507):877–926. doi:[10.1002/qj.49711850705](https://doi.org/10.1002/qj.49711850705)
- Yatagai A, Kamiguchi K, Arakawa O, Hamada A, Yasutomi N, Kito A (2012) APHRODITE: constructing a long-term daily gridded precipitation dataset for Asia based on a dense network of rain gauges. *Bull Am Meteorol Soc* 93(9):1401–1415. doi:[10.1175/BAMS-D-11-00122.1](https://doi.org/10.1175/BAMS-D-11-00122.1)

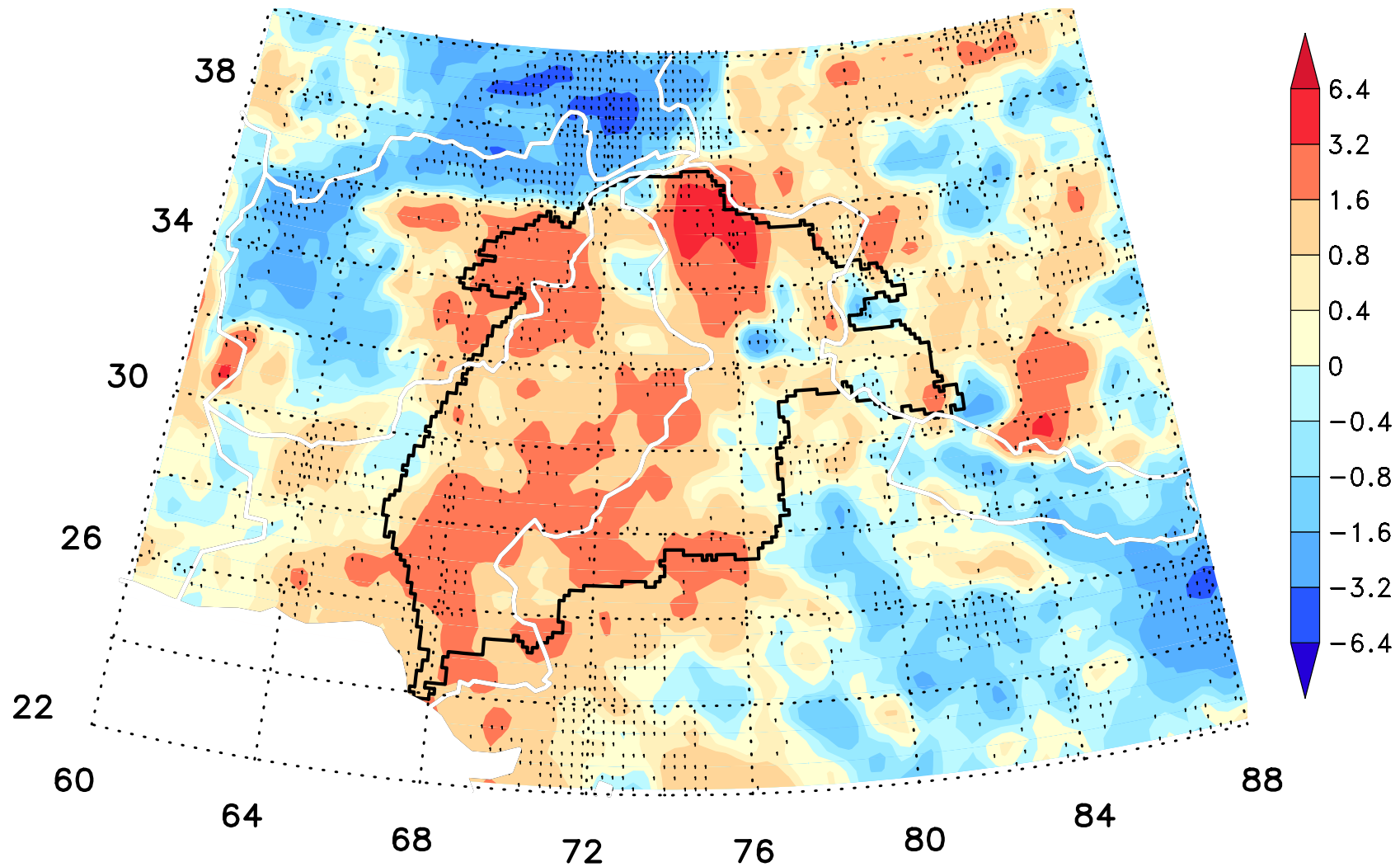




**Auxiliary Figure A1:** Wind at 850 hPa for the heavy rainfall events of a) 12 July 2010 b) 29 July 2010 c) 17 June 2013 and d) 04 September 2014. References for these four events are from Hong et al. (2011), Rasmussen et al. (2015), Vellore et al. (2015) and Lotus (2015) respectively. Wind data is taken from ERA Interim reanalysis. Note the trough-like feature in the upper-level extra-tropical westerlies. Differences in the low-level monsoon southwesterly winds can also be noted among the individual cases.



**Auxiliary Figure A2:** Time series of total count of extreme precipitation over WH [64°-76°E, 28°-40°N] region for APHRODITE (green) and TRMM3B42 (blue) datasets for the common period 1998-2007. These two times series are strongly correlated ( $r=0.97$ ).



**Auxiliary Figure A3:** Spatial map showing trend in frequency count of extreme rainfall events (rainfall  $\geq 99^{\text{th}}$  percentile; unit: count  $[18 \text{ year}]^{-1}$ ) for the TRMM3B42 precipitation datasets for the period (1998-2015). Trend values exceeding the 95% confidence level based on a student's t test (Santer et al. 2000) are marked with dots. The increasing trend of heavy rainfall over the upper Indus basin can be noticed. It is realized that the trends over Northwest India are different as compared to the APHRODITE dataset and will require further investigations.